Proton emission from ^{125}Pm could be observed

Enrico Maglione*
Dipartimento di Fisica e Astronomia "G. Galilei," and Istituto Nazionale di Fisica Nucleare, Via Marzolo 8, I-35131 Padova, Italy

Lidia S. Ferreira†
Centro de Física e Engenharia de Materiais Avançados CeFEMA, and Departmento de Física, Instituto Superior Técnico, Universidade de Lisboa, Avenida Rovisco Pais, P1049-001 Lisbon, Portugal
(Received 21 June 2016; published 19 October 2016)

We perform a feasibility study for the search of proton decay from Pm, the last element without an isotope found, that decays by proton emission in the region of charges between 50 and 83. The behaviors of the half-lives for decay from the ground and possible isomeric states of ^{125}Pm are discussed as a function of deformation, spin of the decaying state, and energy of the emitted proton, indicating the most probable regions of energy where proton radioactivity might be detected. We find that within our predictions, proton decay from ^{125}Pm could be measurable.

DOI: 10.1103/PhysRevC.94.044317

I. INTRODUCTION

Promethium is the only chemical element for which no neutron-deficient isotope that could decay by emitting a proton has been found. Such finding completes the identification of the proton drip line in the region of charges between 50 and 83.

There have been a few attempts in the past at GSI [1], Argonne National Laboratory [2], and Legnaro [3] to measure decay from ^{125}Pm and ^{126}Pm, but they failed, due to the very small production cross sections, implying a low statistic of events, and also possibly as a result of the incapability to detect decays with very small half-lives. Proton radioactive nuclei have been mainly produced in fusion evaporation reactions, with cross sections that can be as low as few tens of nanobarns. Typical values of the half-lives observed for proton emission ranged from tens of microseconds up to hundreds of milliseconds, or even a few seconds [4]. Very often, proton radioactivity is competing with another decay channel, but if proton emission is very fast, it will not be difficult in principle, to observe it, within our present detection limitations. If it is very slow, β decay will occur first, allowing a small branching ratio for proton emission and imposing a constraint of order of seconds on the upper value for the observation of the half-life. Decay to the excited 2^+ of the daughter nucleus could also present in general a very weak proton branch.

Since the discovery of the first proton emitter in the 1970s [5], almost all experiments that followed relied on the double-sided silicon strip detector (DSSD), which allows the exotic nucleus to be implanted in the detector and decay there.

When the nucleus is implanted in the detector, there is a very large signal in the detector during approximately 1 μs, coming from the large energy deposited during the implantation. If the proton is emitted within this time interval, this fast decay event might not be registered because the amplifier is overloaded from the implantation signal, and so the possible detection of the proton will be blocked for a time of order of few μs.

With the recent development of digital signal processing (DSP) [6,7] it is now possible to measure sub-μs half-lives. The nucleus ^{145}Tm [8] provided the first example of such achievement in pulse processing, and a half-life of $\approx 3\,\mu$s was measured. The signals from the detectors were digitally processed using the Digital Gamma Finder, which proved to be a quite useful tool in the following fine structure studies [9]. Recently developed digital-based data acquisition systems (DAQ) [7,10] are faster, with minimal dead time and large capability of handling piled-up signals, and can operate with various detector systems, including DSSD. It is then expected that it will be possible to measure shorter half-lives, allowing us to observe cases where the proton has a larger outgoing energy.

From the above discussion, one can define upper and lower limits for the half-life for proton emission that can be measured, ranging from 10 s to tenths of μs, and this time window can be translated in an energy window available for detection of the outgoing proton. This can perhaps explain why in the mass region of charges below 50, proton radioactivity from the ground state was not observed. In this region, the proton separation energy changes more rapidly than for higher charges; therefore, it becomes quite difficult for the separation energy to be within the window for the energy and angular momentum defined by experimental requirements. Proton emitters should also exist with charges above $Z = 82$, but according to the energy window, the ones that could be observed might be far away from the stability valley and consequently very difficult to produce.

The half-lives for decay depend strongly not only on the energy of the emitted proton but also on the angular momentum of the decaying state and on structure properties, mapped in the spectroscopic factor, and there is a very delicate balance between all these quantities. In the case of decay of a spherical nucleus, this dependence can be very easily illustrated and leads to the energy window depicted in Fig. 1, where the half-lives

*maglione@pd.infn.it
†flidia@ist.utl.pt

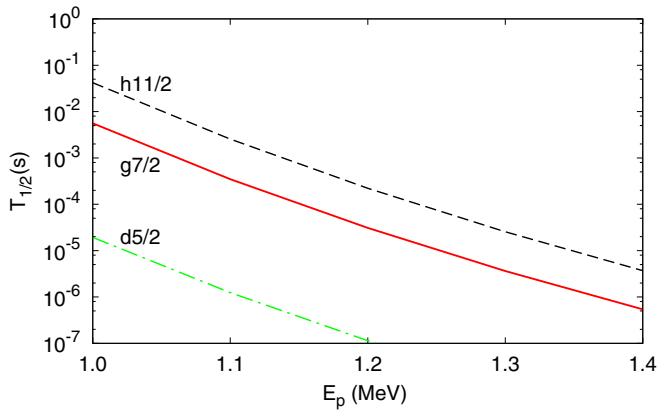

FIG. 1. Half-lives for emission of a proton from different spherical single-particle states in ^{125}Pm, as a function of the proton energy.

for emission of a proton from different single-particle states are plotted as a function of the proton energy. As can be seen, the correlation among angular momentum of the decaying state, proton energy, and half-life is very strong, and only specific combinations between them can fit within the observable window.

Promethium is in the mass region where the negative single-particle parity states are mainly based on the $h11/2$ spherical state, and it is predicted to have a large deformation [11,12]. The proton Fermi surface is located in the low-Ω region of the $h11/2$ shell. For oblate and moderate prolate deformations, the strong coupling model should not work, since the Coriolis interaction is very strong, with respect to the spreading between the energy levels. One thus expects a decoupled band, resulting in rotational alignment [13,14]. In fact, the yrast bands should be built upon a decoupled $h11/2$ proton and consequently might be characterized by a band with the same energy spacings as in the rotational band of the daughter even–even nucleus, independently on the K value of the Nilsson level close to the Fermi surface.

In the same mass region, partial rotational alignment was suggested through the interpretation of the experimental data on proton radioactivity from the ground state of ^{121}Pr [15]. Similar phenomena, for the excited states of ^{125}Pm, might be expected to occur.

For this reason, we have plotted in Fig. 2 the known experimental spectra of odd-even isotopes of Pm in comparison with the spectra of the neighbor even-even isotopes of Nd. One finds that for a large number of neutrons, the deformation is small, and the energy spacings are the same, indicating rotational alignment or a decoupled band, with the $11/2^-$ state as the ground state. With the increase of deformation towards the drip line, a transition starts to the strong coupling case, for which the ground state should be equal to the quantum number K of the Nilsson state.

All these nuclear structure aspects provide strong motivation for the experimental search of ^{125}Pm. Therefore, we have performed a feasibility study for the measurement of decay from this nucleus that might help the search for this emitter by analyzing in detail the dependence on the various quantities that constrain the behavior of the half-life, and branching ratio. The model used is the nonadiabatic quasiparticle model [25], which takes into account the Coriolis coupling, pairing residual interaction, and the spectrum of the daughter nucleus, taken from the experiment, thus including correctly the energies even of the high-spin states.

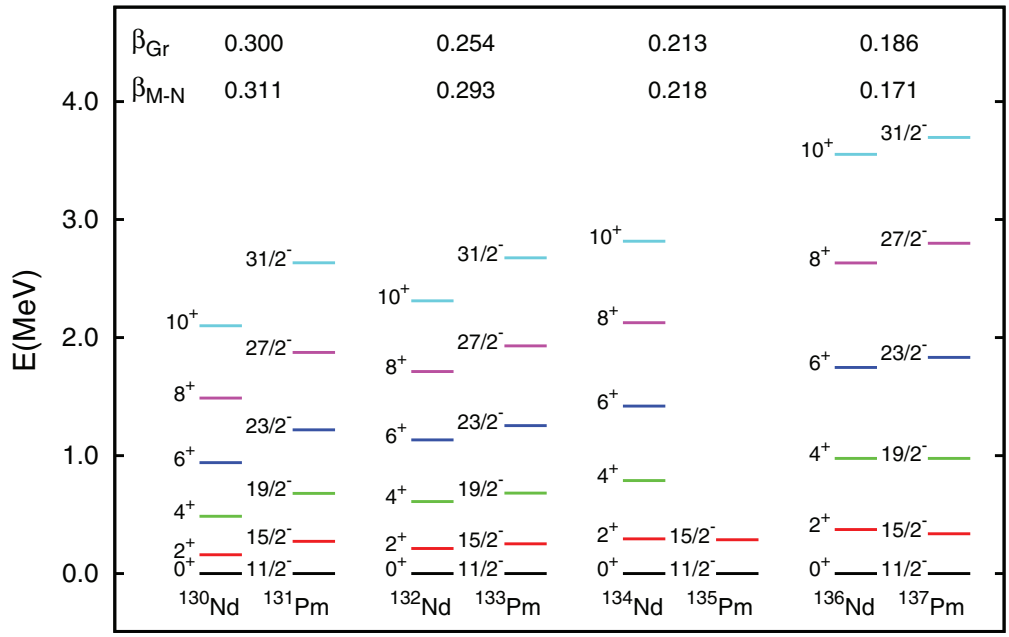

FIG. 2. Experimental ground-state rotational bands of different Nd isotopes, compared to the negative-parity bands in the neighbor Pm nucleus. The quadrupole deformations β_{GR} and β_{MN} assigned to the different nuclei have been calculated using the Grodzins formula [16] and Möller and Nix predictions [11], respectively. The experimental data are taken from Refs. [17–24].

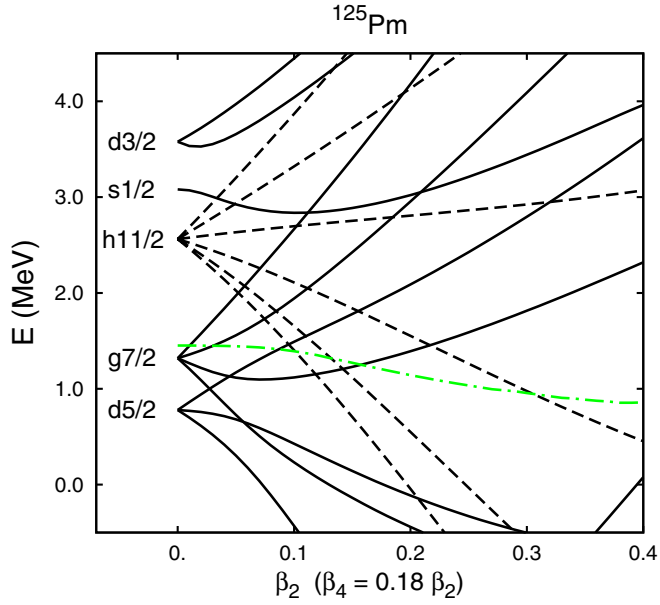

FIG. 3. Nilsson energy levels for protons in ^{125}Pm. The Fermi energy is represented by the green dot-dashed line.

II. RESULTS AND DISCUSSION

For a deformed nucleus, we consider the total Hamiltonian,

$$H = H_{\text{int}} + H_{\text{rot}}, \tag{1}$$

described by the term H_{int}, containing the Nilsson Hamiltonian and the pairing residual interaction, and the rotational Hamiltonian H_{rot}, which includes the spectrum of the core and the coupling of the proton to the core. According to the nonadiabatic quasiparticle model [25], the proton is in a single-particle resonance state, and a correct description of decay requires that the H_{rot} interaction has to be diagonalized between quasiparticle states.

The proton Nilsson resonances in ^{125}Pm were determined using a parametrization for the mean field of Ref. [26], and they are depicted in Fig. 3.

The levels close to the Fermi surface are the most probable candidates for decay, and at low and intermediate deformations, they are the $5/2^+$, $1/2^-$, $3/2^-$, and above $\beta_2 = 0.2$, they are $3/2^+$ and $3/2^-$. However, if the deformation is not too high, the Coriolis interaction becomes very important, and induces a mixing of states that leads to rotational alignment.

Proton emission is a slow process when compared to γ decay; therefore, it will occur only from the ground or an isomeric state. In order to identify the bandhead, we have diagonalized the interaction of Eq. (1) to obtain the energy levels of ^{125}Pm. The calculation was performed first for ^{131}Pm and ^{133}Pm, since their spectra have been observed and could provide a test of our model. The theoretical spectrum of the negative-parity states, relatively to the $11/2^-$ state, is shown as a function of deformation in Fig. 4, in comparison with the experimental one. We have reproduced very well the experimental spectra of these nuclei, for deformations close to the ones of Möller and Nix [11], and we also predict that below the $11/2^-$, there might exist a $9/2^-$, and a $7/2^-$ very close in energy to the $11/2^-$, but due to the low energies of the electromagnetic transitions they might not be easily detected experimentally. In ^{133}Pm the $9/2^-$ was seen just 18 keV above the $11/2^-$ and is reproduced in our calculation.

Since for ^{133}Pm also positive-parity states at even lower energy have been observed, we repeated the calculation for them, and were able to reproduce very well the experimental results, as shown in Fig. 5.

The previous calculation gave confidence for the prediction of the spectrum of ^{125}Pm with our model, which is shown in Fig. 6, for the negative-parity yrast states. Since Möller and Nix predict[11] for this nucleus $\beta_2 = 0.328$ and $\beta_4 = 0.060$ we have taken into account a β_4 dependence of the form, $\beta_4 = 0.18 \times \beta_2$.

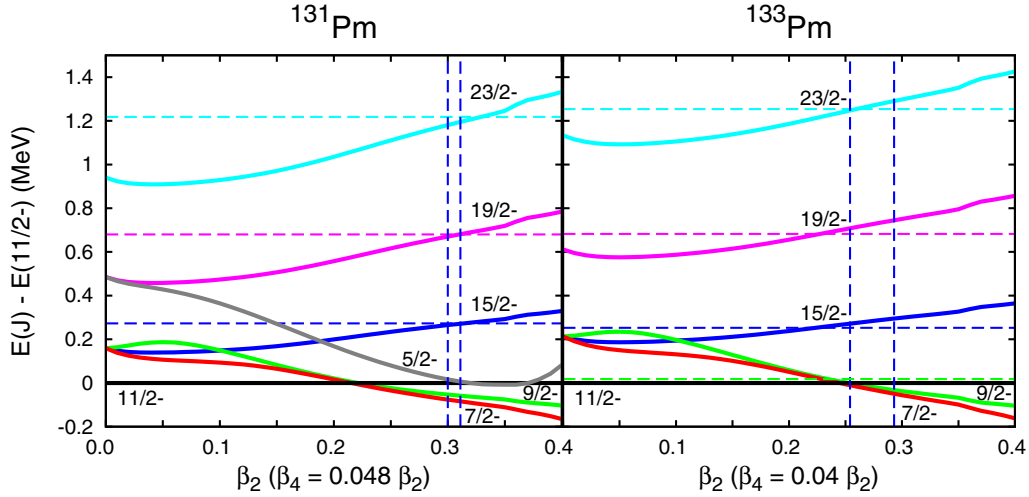

FIG. 4. Energies of the negative-parity states of the Hamiltonian of Eq. (1) with respect to the $J^\pi = 11/2^-$ state for ^{131}Pm and ^{133}Pm, as a function of deformation. The horizontal dashed lines indicate the experimental energies [18,20], and the vertical ones indicate the deformation attributed in Ref. [16] (left) and Ref. [11] (right).

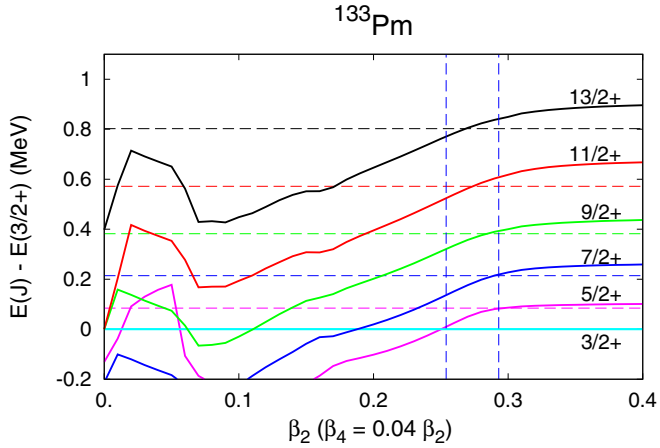

FIG. 5. As in Fig. 4, for the positive-parity states in ^{133}Pm, with respect to the $J^\pi = 3/2^+$ state.

The bunching of levels at zero deformations corresponds to the coupling of the $h11/2$ spherical proton level, to the spectrum of the ^{124}Nd core. Since the spectrum of the daughter nucleus is not known, we have used the experimental spectrum of the close neighbor with $Z = 60$, the nucleus ^{128}Nd [29], which is expected to have essentially the same deformation as ^{124}Nd, thus justifying our choice.

From the analysis of Fig. 6, the lowest negative-parity energy state can be identified as the $11/2^-$ for low deformation, the $7/2^-$ from $\beta_2 = 0.18$, and the $5/2^-$ for a deformation above $\beta_2 = 0.33$.

The exact value of deformation at which the crossing between the $11/2^-$ and $7/2^-$ states occurs depends on the energy of the 2^+ excitation in the core, which is not known, but based on the observation of Fig. 6, one could define an interval for the variation of the deformation encompassing the crossings. Thus, the bandhead for low deformation up to values of $\beta \approx 0.15$–0.25 should be the $11/2^-$; for intermediate deformations, $\beta \approx 0.15$–0.35, it should be the $7/2^-$; and for

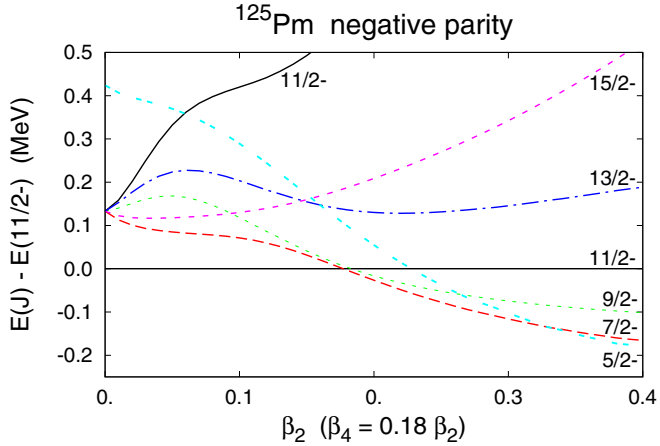

FIG. 6. Energy spectrum of the negative parity states of ^{125}Pm with respect to the $J^\pi = 11/2^-$ state, as a function of deformation.

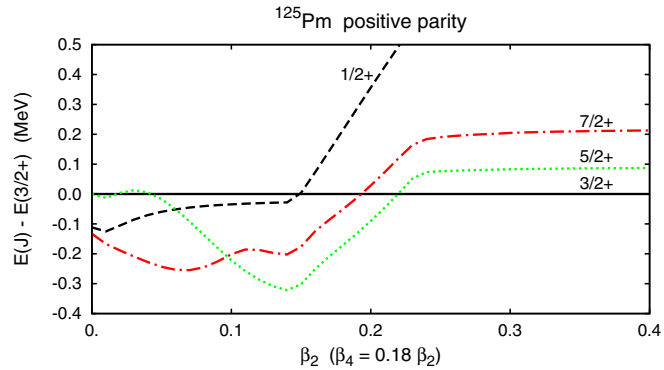

FIG. 7. As in Fig. 6 for the positive-parity states.

larger deformations, above $\beta_2 \approx 0.3$, the $5/2^-$ might be the lowest energy state.

Therefore, for the large deformation $\beta_2 \approx 0.328$ expected for ^{125}Pm [11], the negative-parity state $7/2^-$ or even the $5/2^-$, could be the bandhead. Similar behavior was also observed in the proton emitter ^{121}Pr [15], but in the present study, the $7/2^-$ state was not observed experimentally in ^{131}Pm, and our calculation predicts it at ≈60 keV below the $11/2^-$.

The spectrum of the positive-parity states relative to the $3/2^+$ is shown in Fig. 7 as a function of deformation. For small deformations below $\beta_2 = 0.2$, the energies are quite dependent on the relative energies of the spherical single-particle states. The latter depend strongly on the Wood-Saxon parameters, and small changes in the nuclear radius, or the strength of the spin-orbit interaction, might change significantly the results.

For low deformation, the lowest positive-parity state is the $3/2^+$. The Wood-Saxon we are using places this state at half an MeV below the lowest negative-parity state, and so it should be the ground state, but, as stated above, this energy depends strongly on the position of the spherical $h_{11/2}$ with respect to the positive-parity state, which by itself depends strongly on the strength of the spin-orbit interaction.

To clarify this point, we plot in Fig. 8 the energy difference between the $11/2^-$ and the $3/2^+$ states in ^{133}Pm, and ^{125}Pm, compared with the experimental value measured for ^{133}Pm. The figure clearly shows that the $3/2^+$ and the $11/2^-$ might be very close in energy, with the $3/2^+$ lower for large β_2. However, for the Möller and Nix deformation expected for ^{133}Pm, $\beta_2 \approx 0.28$, the difference between these states is 470 keV, whereas the experimental value is 130 keV, leading to a result overestimated by ≈340 keV. For ^{125}Pm at $\beta_2 \approx 0.33$, this difference is 550 keV, and if the same overestimation is attributed, the difference in energy between the $11/2^-$ and the $3/2^+$ states might be ≈210 keV. If instead it is the $7/2^-$ the bandhead, the same argument gives a difference between the $3/2^+$ and the $7/2^-$ of ≈75 keV, making the electromagnetic transition from the negative-parity state to the positive-parity one almost impossible, and suggesting that the $7/2^-$ could be an isomeric state.

Consequently, looking at the energies and assuming that ^{125}Pm has a deformation $\beta > 0.2$ we can expect that most probably the ground state is the $3/2^+$. However, if the deformation is below $\beta = 0.2$ there could be an isomeric

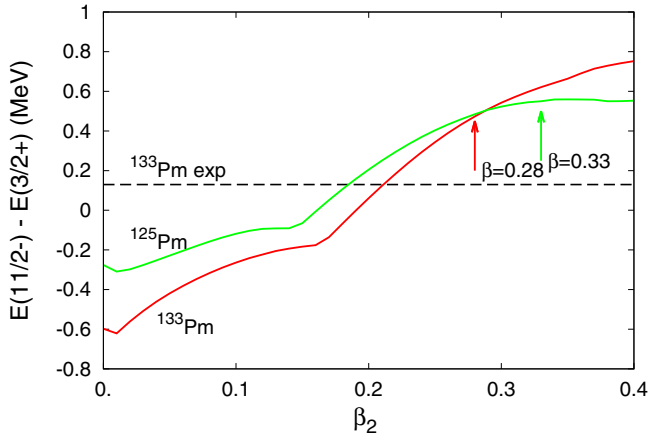

FIG. 8. Energy difference between the $11/2^-$ and the $3/2^+$ states in ^{133}Pm (red line) and ^{125}Pm (green line). The dashed line indicates the experimental value for ^{133}Pm, and the arrows define the energy difference at the expected deformation predicted in Ref. [11].

$11/2^-$ state that has a small chance to be the ground state. But for a larger deformation $\beta \approx 0.3$ there is a small chance that the $7/2^-$ or $5/2^-$ could be isomeric states or even the ground state.

In order to calculate the half-life for proton emission, one should discuss what would be expected for the value of the energy of the outgoing proton. For this, we make a comparison in Fig. 9, between the mass formula predictions of Liran and Zeldes [28] and Möller and Nix [27] and the experimental values for the known proton emitters, in order to extrapolate a Q value for ^{125}Pm. In the region around ^{125}Pm, the calculations of Ref. [28] overestimate by ≈150–300 keV the experimental values, as can be seen from Fig. 10, and since it would predict a proton separation energy of 1.450 MeV for ^{125}Pm, we expect an energy between 1.15 and 1.3 MeV for the ground state of positive parity and between 1.225 and 1.5 MeV for an isomeric state of negative parity. The predictions of the calculations of Ref. [27] represent a more erratic behavior, since they agree in some regions with the ones of Ref. [28] and underestimate the data in others, so it is difficult to extract any conclusion from them.

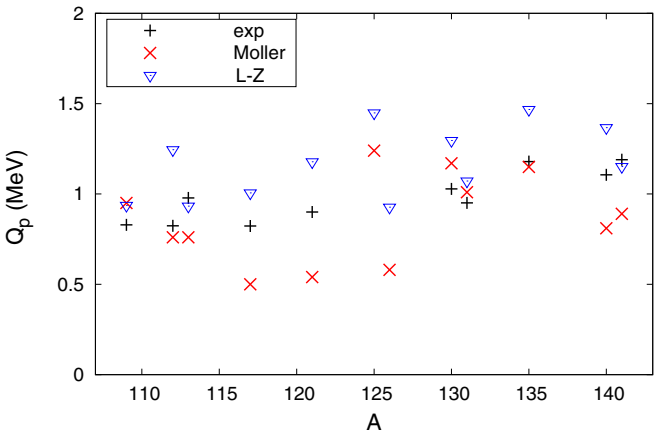

FIG. 9. Q values of the proton emitters observed experimentally, and the mass formula predictions of Refs. [27,28].

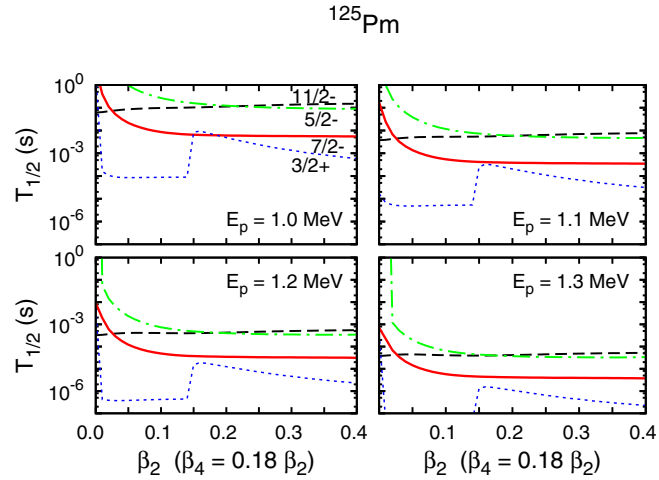

FIG. 10. Half-lifes for decay from the states $3/2^-$, $5/2^-$, $7/2^-$, and $11/2^-$ at different proton energies.

The half-lives for decay from the various states discussed above are presented in Fig. 10 as a function of deformation, for different energies available for the outgoing proton.

It can be seen that there is a strong dependence on the Q value, but the half-lives for decay from states that we found to be the bandhead at a specific deformation correspond to times that span from the order of a tenth of the microseconds up to few milliseconds, which are measurable. The half-life of the $3/2^+$ state has a jump around $\beta = 0.14$, but this behavior is due to a crossing of levels, as can be seen in the Fig. 7, which completely changes the wave function of the nucleus and consequently the results for the calculated observables in this region.

We have also calculated the fine structure for decay to the 2^+ of ^{124}Nd, presented in Fig. 11 and found some very large values of order of 30–70% for very small deformations and below 30% at the expected deformation. Only the $7/2^-$ has a very small branching ratio. However, it should be noted that these values will obviously depend strongly on the energy of the 2^+ in the daughter nucleus, which is not known. In our

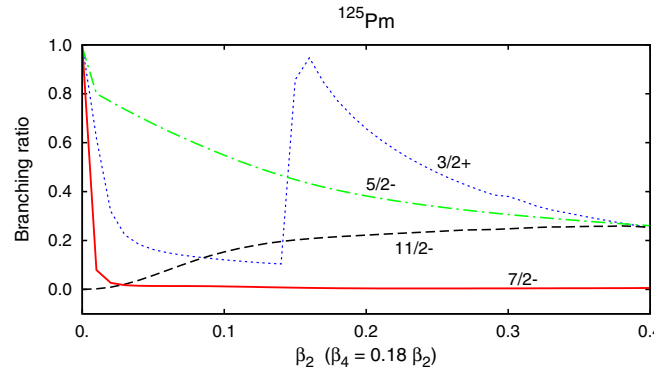

FIG. 11. Branching ratio for decay from different single-particle states, to the 2^+ state in ^{124}Nd.

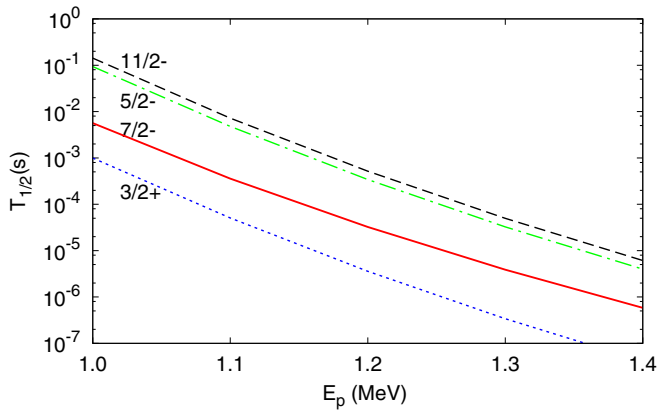

FIG. 12. Half-life for decay of ^{125}Pm from different single-particle states as a function of the proton energy, at a deformation $\beta = 0.33$.

calculation we have used the energy observed in ^{128}Nd, but if this energy is higher, the half-life would became longer and the branching ratio smaller.

Finally, the half-life for decay of ^{125}Pm from the different single-particle states, which according to our calculation are the most probable decaying states, is shown in Fig. 12 as a function of the proton energy, for the predicted deformation [11]. Given the estimates for the proton separation energy mentioned before, and the available sensibility of present detectors, the half-life is within the energy window that could be observed.

A similar calculation for the half-lives and branching ratios performed with universal parametrization of the nuclear interaction [30] gave essentially the same results, thus not altering our predictions.

III. CONCLUSIONS

In conclusion, proton emission from ^{125}Pm could be observed with an experimental apparatus able to measure half-lives longer than 0.2 μs. These decays could be detected with quite reasonable Q values of less than 1.3 MeV, if the decaying state is the $3/2^+$, or lower than 1.5 MeV for decay from negative-parity states. This study would allow also to observe a quite large branching ratio.

ACKNOWLEDGMENTS

We thank D. Seweryniak and F. Soramel for useful discussions.

[1] P. O. Larsson *et al.*, Z. Phys. A **314**, 9 (1983).
[2] P. Munro, DPhil thesis, School of Physics, University of Edinburgh, 2006 (unpublished).
[3] F. Soramel *et al.*, AIP Conf. Proc. **681**, 18 (2003).
[4] A. A. Sonzogni, Nucl. Data Sheets **95**, 1 (2002).
[5] J. Cerny *et al.*, Phys. Lett. B **33**, 284 (1970).
[6] R. Grzywacz *et al.*, Nucl. Inst. Meth. B **204**, 649 (2003).
[7] J. Anderson *et al.*, IEEE Trans. Nucl. Sci. **56**, 258 (2009).
[8] C. R. Bingham *et al.*, Nucl. Inst. Meth. B **241**, 185 (2005).
[9] K. P. Rykaczewski *et al.*, AIP Conf. Proc. **681**, 11 (2003).
[10] J. T. Anderson *et al.*, *Nuclear Science Symposium and Medical Imaging Conference (NSS/MIC)* (IEEE, Anaheim, CA, 2012), pp. 1536–1540.
[11] P. Möller, J. R. Nix, W. D. Myers, and W. J. Swiatecki, At. Data Nucl. Data Tables **59**, 185 (1995).
[12] G. A. Lalazissis, D. Vretenar, and P. Ring, Nucl. Phys. A **650**, 133 (1999).
[13] F. S. Stephens, Rev. Mod. Phys. **47**, 43 (1975).
[14] F. S. Stephens, R. M. Diamond, J. R. Leigh, T. Kammuri, and K. Nakai, Phys. Rev. Lett. **29**, 438 (1972).
[15] M. C. Lopes, E. Maglione, and L. S. Ferreira, Phys. Lett. B **673**, 15 (2009).
[16] L. Grodzins, Phys. Lett. **2**, 88 (1962).
[17] B. Singh, Nucl. Data Sheets **93**, 33 (2001).
[18] Yu. Khazov, I. Mitropolsky, and A. Rodionov, Nucl. Data Sheets **107**, 2715 (2006).
[19] Yu. Khazov, A. A. Rodionov, S. Sakharov, and B. Singh, Nucl. Data Sheets **104**, 497 (2005).
[20] Yu. Khazov, A. Rodionov, and F. G. Kondev, Nucl. Data Sheets **112**, 855 (2011).
[21] A. A. Sonzogni, Nucl. Data Sheets **103**, 1 (2004).
[22] B. Singh, A. A. Rodionov, and Y. L. Khazov, Nucl. Data Sheets **109**, 517 (2008).
[23] A. A. Sonzogni, Nucl. Data Sheets **95**, 837 (2002).
[24] E. Browne and J. K. Tuli, Nucl. Data Sheets **108**, 2173 (2007).
[25] G. Fiorin, E. Maglione, and L. S. Ferreira, Phys. Rev. C **67**, 054302 (2003).
[26] H. Esbensen and C. N. Davids, Phys. Rev. C **63**, 014315 (2000).
[27] P. Möller, J. R. Nix, and K.-L. Kratz, At. Data Nucl. Data Tables **66**, 131 (1997).
[28] S. Liran and N. Zeldes, Atomic Data Nucl. Data Tab. **17**, 431 (1976).
[29] Z. Elekes and J. Timar, Nucl. Data Sheets **129**, 191 (2015).
[30] J. Dudek, Z. Szymanski, T. Werner, A. Faessler, and C. Lima, Phys. Rev. C **26**, 1712 (1982).